

## Diffusion-limited island decay of PTCDA on Ag(100): Determination of the intermolecular interaction

Julian Ikononov,\* Christoph H. Schmitz, and Moritz Sokolowski

*Institute for Theoretical and Physical Chemistry, University of Bonn, Wegelerstr. 12, 53115 Bonn, Germany*

(Received 10 March 2010; published 25 May 2010)

The coarsening of two-dimensional islands of the model molecule perylene-3,4,9,10-tetracarboxylic acid dianhydride adsorbed on the Ag(100) surface was investigated by scanning tunneling microscopy. The islands have a quadratic equilibrium shape with rounded corners. The decay curves (island area versus time) can be understood by the classical continuum model according to the Ostwald theory. In the limit of well-separated islands, the asymptotic power law ( $t^\alpha$ ) exhibits an exponent  $\alpha=0.67 \pm 0.05$ . This reveals that the coarsening is diffusion limited and that no interfacial barrier exists between island edge sites and terrace sites. From numerical simulations on an ensemble of islands, using the mean-field approach, we determine the average line tension of the island edge at  $51 \pm 5$  meV per molecule. Here from we deduce a next-neighbor intermolecular interaction of  $102 \pm 10$  meV.

DOI: [10.1103/PhysRevB.81.195428](https://doi.org/10.1103/PhysRevB.81.195428)

PACS number(s): 68.43.Jk, 68.37.Ef, 34.20.Gj

### I. INTRODUCTION

Island ripening, island coalescence, and cluster diffusion are examples of surface kinetic processes that have so far been studied in detail mainly for metals and semiconductors.<sup>1,2</sup> However, over the last years, thin films of larger organic molecules, in particular with semiconducting properties, which are vacuum deposited on different inorganic substrates have gained attention, under both scientific<sup>3,4</sup> and technological aspects.<sup>5</sup> In this context, information about basic mechanisms and relevant time scales of kinetic processes of organic molecules on inorganic substrate surfaces is important, e.g., to understand and control film growth processes or to tailor the dimensions of surface supported organic nanostructures.

Here we report on an investigation on the organic prototype molecule perylene-3,4,9,10-tetracarboxylic acid dianhydride (PTCDA) on the Ag(100) surface. The aim was to obtain microscopic energetic parameters from the island ripening at low overall coverages. In particular, we were able to derive information from the island decay on the diffusion field between the islands, the absence of a possible interfacial barrier for molecules at the island edges, and on the line tension per molecule at the island edge. This latter parameter is interesting insofar as it gives access to the lateral intermolecular interaction energy between adsorbed PTCDA molecules within an island, which is an important microscopic parameter in this system.

Before we turn to our specific example, we briefly resume some aspects of the Ostwald ripening theory for islands on surfaces which appears to be applicable here.<sup>6,7</sup> In general, the Ostwald theory describes the growth or ripening of large islands on the expense of smaller ones which exhibit a higher chemical potential due to the line tension of the island edges. There exist two limiting cases with different kinetics. The *attachment-limited* (or interface limited) ripening occurs in those systems where an energetic barrier for the transition of a particle between a site at an island edge and a site on the surface (interfacial or attachment barrier) exists. The origin of this barrier is related to the specific incorporation process

of the particle at the island edge, as the rearrangement of bonds, e.g., for semiconductors surfaces as Si(001).<sup>8</sup> In this case the diffusion rate of the particles away from or to the islands is higher than the attachment-detachment rate ( $\kappa_{\text{Diff}} \gg \kappa_{\text{AD}}$ ).<sup>6</sup> Hence, particles which have once detached from an island edge are transferred fast due to a diffusive motion with a high rate. As a consequence, the particle density on the surface is uniform and the island ripening is not influenced by the specific placement of the islands relative to each other. As a result, the asymptotic decay of the island area is linear in time.<sup>1,2,9</sup>

In the case of the *diffusion-limited* decay, the diffusion rate of the particles away from or to the islands is smaller than the attachment-detachment rate ( $\kappa_{\text{Diff}} \ll \kappa_{\text{AD}}$ ).<sup>6</sup> The detached particles distribute themselves only slowly on the surface and a nonconstant particle density (diffusion field) with a gradient, pointing toward the island edges, is built up. For a circular island the equilibrium density value  $\rho_r$  directly in front of the island edge is related to the island radius  $r$  by the Gibbs-Thomson relation,

$$\rho_r = \rho_\infty \exp\left(\frac{\gamma \Omega}{k_B T r}\right), \quad (1)$$

with  $\rho_\infty$  denoting the equilibrium density of an infinitely large island,  $\gamma$  denoting the average island edge tension, and  $\Omega$  denoting the area per molecule. As a consequence, the growth or decay of an island is influenced by the local arrangement of other islands in its neighborhood. Neglecting the influence of possible neighbor islands, the asymptotic decay kinetics of an island area is given by power law  $\sim t^\alpha$  of the remaining life time  $t$  with a time exponent of  $\alpha=2/3$ .<sup>1,2</sup>

Metal and semiconductor islands have already been investigated on a wide range of surfaces.<sup>10–19</sup> The ripening of molecular clusters or island was studied for C<sub>60</sub> on Si(110) (Ref. 20) and for rubrene on sapphire.<sup>21</sup> An experiment which bears some similarity, is the study of the island density of PTCDA on Ag(111) by Schmidt *et al.*,<sup>22</sup> which, however, yields mainly information on the nucleation process.

The system PTCDA on Ag(100) was chosen for these experiments for several reasons. First of all, PTCDA on Ag(100) orders in a commensurate highly symmetric quadratic superstructure with two molecules per unit cell.<sup>23</sup> There are two molecules in the unit cell in a T-shape arrangement. The charge distribution corresponds to that of a quadrupole with negatively charged anhydride groups and a positively charged perylene core. The attractive intermolecular interaction between next-neighbor molecules likely includes both electrostatic and substrate mediated components, similar as it was reported for PTCDA on Ag(111).<sup>24,25</sup> The long axes of the molecules are oriented parallel to the close-packed directions of the Ag(100) surface. The unit cell covers 16 unit cells of the Ag(100) surface. It is illustrated in Fig. 2(d)(below). Second, PTCDA/Ag(100) was chosen because, likely due to the fairly large corrugation of the Ag(100) surface, isolated two-dimensional PTCDA islands with an equilibrated shape can be prepared on terraces by evaporation at low temperatures. This is for instance not possible on Ag(111), where island nucleation occurs always at substrate steps, even at low temperatures.

## II. EXPERIMENT

The experiments were performed in an ultrahigh vacuum chamber with a base pressure below  $2 \times 10^{-10}$  mbar, equipped with a beetle-type STM from RHK. The PTCDA molecules were deposited by thermal evaporation from a Knudsen cell. At room temperature, PTCDA molecules are rather mobile on the Ag(100) surface and form islands that are attached to the steps.<sup>23</sup> This was undesirable for the present decay experiments. Therefore the deposition was performed at low sample temperatures of about 120 K where the mobility of the molecules on the surface is much smaller and island nucleation occurs also on the terraces. The flux from the Knudsen cell was about 2 monolayers (2 ML) per min. The optimal coverage for these experiments was about 10% of a monolayer. Consequently, we used only small deposition times of about 3 s. We define the ideal coverage of the monolayer structure, as defined in Ref. 23 as 1 monolayer (1 ML). For larger coverages, island coalescence occurred, for smaller coverages, only small islands with small lifetimes were present. After deposition, the sample was then transferred from the preparation to the STM chamber without breaking the vacuum. The final measurements were performed at room temperature, typically starting 2–3 h after the preparation. Using this routine, the STM measurement usually started on a surface with small isolated PTCDA islands on the terraces.

Long series of STM images, lasting over several hours, were recorded in order to monitor the island decay process. For this purpose the STM had to be in a very stable condition, e.g., with practically zero drift. This could be so far achieved only at room temperature, where all experiments were performed. The island areas as a function of time were computed from the STM images by a home-made software. The error depends on the lateral resolution and is estimated to be typically less than the area of two molecules.

An important question for this kind of STM measurements concerns the role of the tip-molecule interactions,

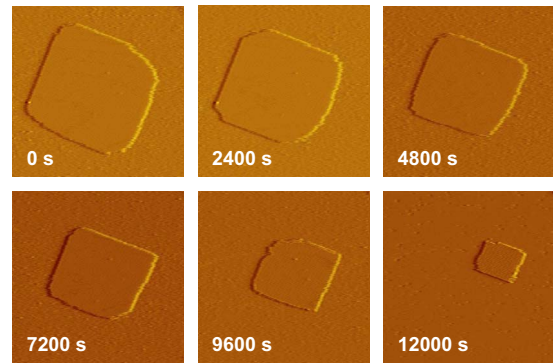


FIG. 1. (Color online) Sequence of STM images ( $120 \times 120$  nm<sup>2</sup>) of a PTCDA island decaying with time. The times are indicated on the images. At  $t=0$  s, the island area is equal to 5678 nm<sup>2</sup> which corresponds to 4253 molecules. The island disappears at  $t_0=12088$  s. Images were taken in constant current mode.  $I_{sp}=23.1$  pA,  $U_b=1.70$  V. One image was recorded within 4 min.

which might distort the result, e.g., by tip-induced dragging of molecules. From independent measurements on this system, we were able to quantify the influence of the tip on the PTCDA molecules.<sup>26</sup> It was found that, for measuring with bias voltages  $U_b$  between 1.5 and 2.0 V (at the sample) and set point currents  $I_{sp}$  less than 100 pA, the tip influence on the molecules appears to be negligible.

## III. RESULTS AND DISCUSSION

### A. Equilibrium shape of the islands

Figure 1 illustrates a time series of STM images showing the decay of one PTCDA island. Generally PTCDA islands on Ag(100) exhibit a quadratic shape with rounded corners. At the beginning of the STM investigations, such quadratic islands were found to be homogeneously distributed on the surface, having typical diameters of 50–100 nm (at room temperature). Interestingly, the island edges are rather straight; they follow the [100] directions of the Ag(100) substrate. They consist of a row of PTCDA molecules with an orientation that alternates by 90° from molecule to molecule. This can be seen in the STM images in Figs. 2(a)–2(c) and is illustrated in the schematic drawing in Fig. 2(d). We note that metal islands at finite temperatures have typically only *quasi-straight* edges,<sup>2,27</sup> which should say that there is a significantly larger number of kinks on metal island edges compared to PTCDA islands.

The observed quadratic shape of the islands is the equilibrium shape since it is maintained during the island decay (see Fig. 1) and since it is also the shape of the islands that grow during the ripening process (not shown here). From the island shape we can hence conclude that the straight island edges along the [100] directions correspond to pronounced minima in the island edge energy. This is due to the fact that for these island edges each molecule at the island edge is bonded to three neighbor molecules via bonds between the O-containing anhydride groups with a negative partial charge and the perylene cores with a positive partial charge [see Fig. 2(d)]. Hence, with respect to a molecule within an island,

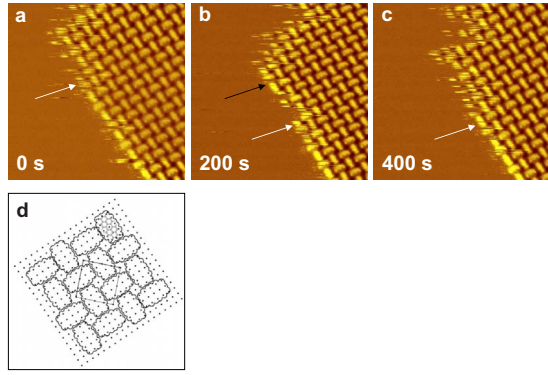


FIG. 2. (Color online) [(a)–(c)] Sequence of STM images of an island edge during island decay. These STM images were measured at constant height mode for better resolution. The times are indicated on the images. The thin bright lines close to the edge result from molecules which attach/detach during the scanning of the STM image. The white arrows indicate the temporal end of the detaching row of molecules. The black arrow points to molecules which temporarily attach to the island edge.  $U_b=1.7$  V. Initial set point current on the Ag(100) surface  $I_{sp}=35.4$  pA. (d) Hard sphere model of the ordered structure of PTCDA on the Ag(100) surface within the island.

which is bonded to four next neighbors, only one intermolecular bond is broken at the island edge. We note that we could not observe any island diffusion, as it was observed for adatom islands<sup>28</sup> or vacancy islands on metals.<sup>17</sup>

**B. Detaching of molecules from islands**

The PTCDA molecules show an interesting mechanism for detaching from the island edges. As noted above, the island edges are almost perfectly straight during the decay process. The molecules positioned at the ends of the island edge, i.e., at the rounded corners, are less coordinated to other PTCDA molecules. Hence they have a higher probability to detach and the detaching of the molecular row that forms the island edge typically starts at a corner of an island. Then the frontier of detaching molecules, which is in principle a kink in the island edge, runs along the island edge. Since the detaching occurs rather slowly, the process can be followed in detail by STM. This is illustrated in Fig. 2, which shows a sequence of STM images where a row of molecules detaches stepwise from the island corner at the top of the image to the bottom.

Evidently, the detachment is a very dynamic process and includes several detachment and reattachment cycles until a molecule has finally departed from the island edge. This can be seen in Fig. 2. Molecules which fluctuate between the terrace and the island edge (which detach and reattach) during the STM scanning process are imaged only by individual bright scan lines with intermittent dark lines (resulting from their absence). Those molecules that are permanently at the island edge are imaged as compact objects, as like those within the island.

In Fig. 2, the white arrow indicates approximately the frontier between fluctuating and resting molecules. Comparing Figs. 2(a) and 2(b) it can be seen that this frontier moves

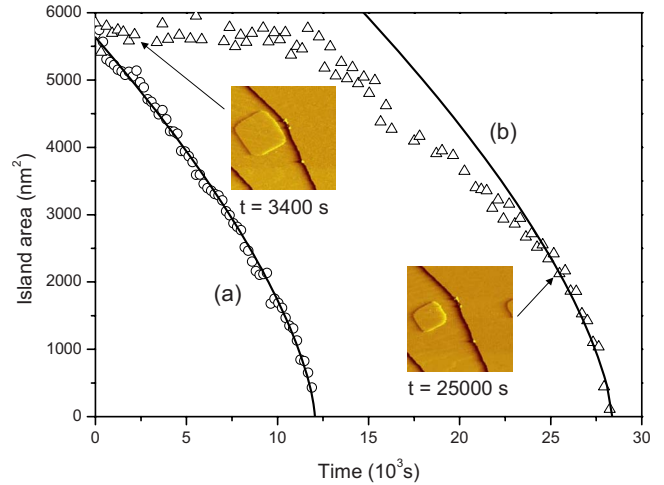


FIG. 3. (Color online) Time evolution of the island area for two exemplary PTCDA islands. Curve (a) represent the area of an island isolated on a large terrace, curve (b) that of an island on a small terrace limited by the steps. The solid lines are fits of the data with an exponent  $\alpha=0.67$ . The insets show STM images of the island (b). Respective images of the island (a) are displayed in Fig. 1.

downward along the island edge. In Fig. 2(b) some additional molecules appear to have reattached to the island above the white arrow (indicated by the black arrow). However, as these are not imaged as compact objects, but with several dark lines, it can be concluded that these molecules are not permanently at the island edge. They perform several attachment-detachment jumps during the scanning process and finally this unstable group of molecules disappears, as seen in Fig. 2(c).

During the overall process there are only very few occasions where we observed attachment of a single molecule to an island edge. Moreover, we did not observe molecules which spontaneously detach from an island edge, leaving a vacancy behind. For the attachment and reattachment processes there is always a kink position involved. As a result, the PTCDA islands exhibit straight edges during the entire decay process.

**C. Decay curves**

Figure 3 shows plots of the island area versus time for two different decaying islands [(a) and (b)]. The island (a) is situated on a larger terrace with no smaller neighbor islands within a distance of 100–200 nm. Corresponding images of the decay are displayed in Fig. 1. For this scenario, where the diffusion field of neighboring islands can be neglected, the Ostwald theory predicts an asymptotic behavior given by a linear dependence in time for an attachment-limited decay, and by a power law  $(t_0-t)^\alpha$  with  $\alpha=2/3$  for a diffusion-limited decay. As illustrated in Fig. 3 for two examples, decay curves of 12 different islands were fitted with the function,

$$A = C(t_0 - t)^\alpha, \tag{2}$$

where  $A$  is the island area and  $C$  is a constant which also depends on the temperature.<sup>2</sup> The exponent was determined

as  $\alpha=0.67 \pm 0.05$ . This indeed agrees very well with the expectation for a diffusion-limited case and indicates that this situation applies here. The good agreement might indicate that the approximations which are required for this asymptotic power-law behavior, e.g., a small line tension and a constant diffusion field, are well fulfilled here (see Ref. 14).

As a consequence, the diffusion fields have in general to be considered and the detailed time dependence of the decay curves is influenced by the local environment of the specific islands. Only in the limit when the island sizes fall considerably below the distance to the next-neighbor island, the asymptotic power-law kinetics is reobtained. Hence, for the island (b) in Fig. 3 and the islands 4–7 in Fig. 4 (discussed below) the decay curves could only be fitted in the last stage of their decay when the island size is already smaller than the other islands in near vicinity.

Compared to the island (a), the situation for the second island (b) (Fig. 3) is interestingly different. This island is situated on an elongated terrace, confined by two about parallel steps of the Ag(100) surface (see insets). This has a considerable influence on the decay. At the beginning, the island decreases only very slowly and the time dependence of the area deviates strongly from the expected power law. Only at the end of the decay, the  $A(t)$  curve can be fitted with the expected exponent of  $2/3$  (as shown in Fig. 3). The deviation from the theoretical curve is similar to that which is expected for a larger island within an ensemble of islands where a high local particle density around the large island is maintained by the more rapid decay of the smaller islands in its neighborhood (see below).<sup>2</sup>

For the island (b) we explain this by two effects: (a) the PTCDA molecules are not adsorbed at the Ag-steps sites but are reflected back into the terraces and (b) that no transport of the PTCDA molecules across the Ag(100) substrate steps occurs. Hence the steps create an effective partial confinement for the molecules. As a consequence, the local surface area around the island will be high and a strong reattachment rate causes that the island size decreases only very slowly. Only in the direction parallel to the steps, mass transport exists. When the size of the island is much smaller than the terrace width, e.g., the Ag step edges are relatively far away from the island, the decay process follows again the theoretically predicted time dependence (see Fig. 3, curve b).

We note that a similar effect is not present for coarsening of metal islands because there the atomic steps of the substrate are equivalent to islands with infinite radii, and all atoms detached from the decaying island adsorb at the steps. This effect reduces significantly the concentration of adatoms on the surface, and quantitatively the decay of a metal island close to steps is similar to that which is observed for an adatom island inside a large vacancy pit.<sup>2,29</sup> It should also be noted that the mirrorlike behavior of the steps for PTCDA is not in contrast to the observation of island nucleation at step sites under deposition at room temperature.<sup>23</sup> The reason is that a much higher temporary particle density is achieved under an external flux, which can lead to stable nuclei at the steps under these conditions.

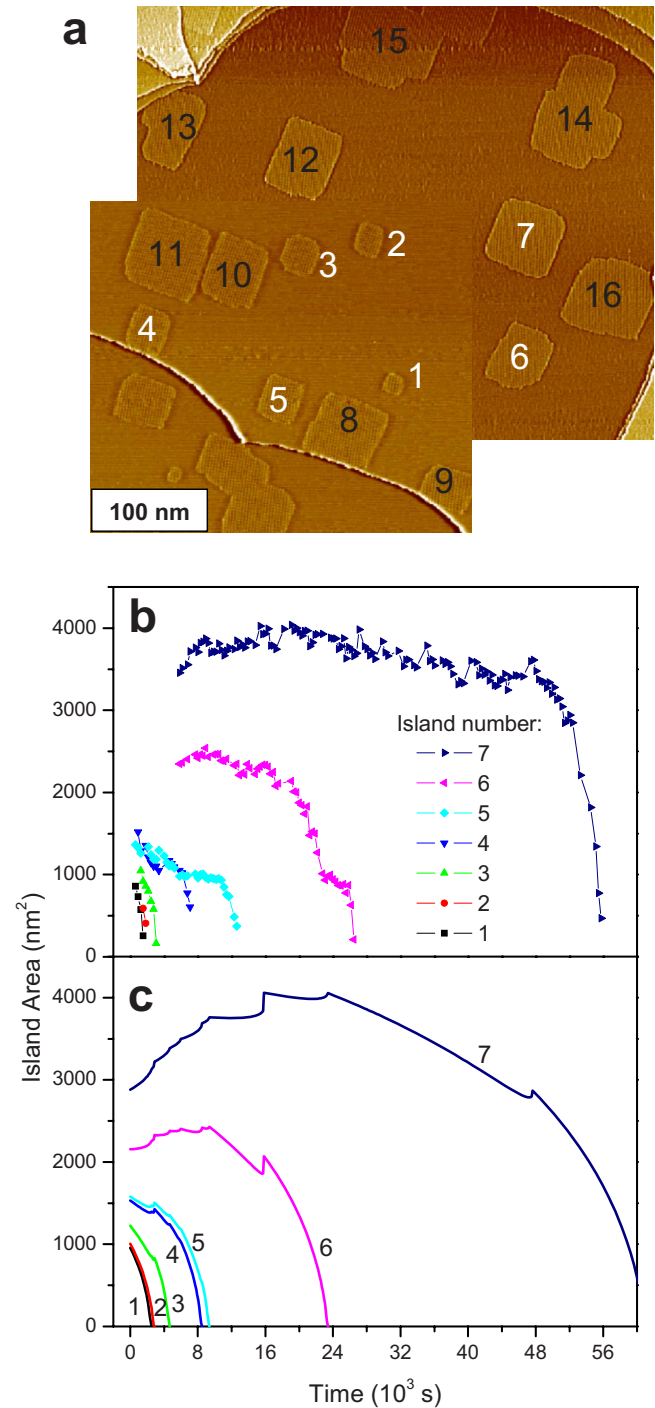


FIG. 4. (Color online) (a) STM image of an ensemble of PTCDA islands on a Ag(100) terrace.  $I_{sp}=25.2$  pA,  $U_b=1.70$  V. The studied islands are numbered (see the text for explanation). (b) Area versus time plots of seven islands. (c) Area evolution of the seven islands simulated within the mean-field approach. For further details see text.

#### D. Simulation of the decay of an ensemble of islands

For a further evaluation of the physical parameters of the island decay we performed a numerical simulation of the decay curves of an ensemble of islands. The start situation is shown in Fig. 4. In this case, several islands of different size

are located on one terrace [Fig. 4(a)]. Our data allowed the extraction of the decay curves for the islands 1–7 (white numbers), which are shown in Fig. 4(b). For the other islands (black numbers), the area determination was incomplete since these islands drifted out of the STM image field during the observation time (15 h) before the decay was completed.

As seen in Fig. 4(a), the smaller islands decay more rapidly. Typical for the situation of a diffusion-limited decay is the mass transport from the smaller to the larger islands.<sup>30,31</sup> This transport cannot directly be observed by STM, but it can indirectly be deduced from the area-time analysis shown in Fig. 4(b) for the seven smallest islands of Fig. 4(a). The islands 1–3 decay monotonically, whereas the islands 4–7 are influenced by the presence of the smaller islands on the terrace and their respective areas show a nonmonotonic behavior until the smaller islands have vanished. The island 7 even grows at the very beginning, indicating a high flux of molecules from the smaller islands in its neighborhood to this island. The decay curves of the island 4 and 5 show a shoulder at about the time when the islands 1 to 3 and the island 4 disappear, respectively, which results from the rapid decay of the latter islands that are smaller than  $\sim 300$  nm<sup>2</sup> (i.e., contain less than 300 molecules). At this stage of decay, these small islands have a high chemical potential leading to a temporary high local density of molecules on the surface that is adsorbed from the larger islands. The whole situation is typical for the diffusion-limited case and is also often observed for the coarsening of metal islands.<sup>2</sup>

We have simulated the experimentally obtained decay curves modeling the diffusion field by a mean-field approach. The method was described by Morgenstern *et al.* in Ref. 31. It was used to simulate the decay of Ag adatom islands on Ag(111). Within this approach the change in the island area is given by

$$\frac{dA}{dt} = -\frac{2\pi\Omega D}{\ln \xi}(\rho_r - \bar{\rho}), \quad (3)$$

whereby  $D$  is the diffusion constant and  $\ln \xi$  is the so-called screening length.<sup>7,32</sup> This parameter describes the local variation in the diffusion field around an island and is a function of the island size; within the mean-field theory it is considered as a constant. Whether an island grows or decays depends on the sign of  $(\rho_r - \bar{\rho})$ , whereby  $\rho_r$  denotes the molecule density directly in front of the edge of an island with radius  $r$  and  $\bar{\rho} = \frac{1}{n} \sum_{i=1}^n \rho_r^i$  the averaged (mean-field) density. The molecule density  $\rho_r$  is given by Eq. (1).

We calculated the decay curves of the ensemble of 16 PTCDA islands situated on the large terrace [Fig. 4(a)] by a numerical integration of Eq. (3) using time steps of 120 s (which are smaller than the time between two consecutive STM images). The input parameters were the positions (centers of mass) and the initial areas of the 16 islands. We varied two parameters to adapt the simulated curves to the experimental ones: the island edge line tension  $\gamma$  in Eq. (1) and the factor  $D\rho_\infty/\ln \xi$  in Eq. (3) [ $\rho_\infty$  enters via  $\bar{\rho}$  in Eq. (3) via Eq. (1)]. The island shapes were assumed as circles in the calculation. In order to account for their quadratic shape in reality,

the obtained value for the line tension was corrected by a shape factor  $2/\sqrt{\pi}$ .<sup>33</sup>

The simulated curves for the seven islands, discussed above, are shown in Fig. 4(c). Considering that the used model is rather simple, the agreement with the experimental data is rather good. According to Morgenstern *et al.*<sup>31</sup> the mean-field approach is applicable to the diffusion-limited case only to some extent since it underestimates the spatial distribution of the islands. Indeed, all decay curves of the PTCDA islands are well reproduced by the calculation with the exception of that of the island 5 for which the simulation predicts a faster decay compared to the experiment. The reason is that this island is surrounded by smaller islands: 1, 2, 3, and 4 [see Fig. 4(a)], which due to their sizes decay more rapidly and act as sources for molecules that are adsorbed by island 5. This specific neighborhood effect is not accounted in the simulation, explaining the variation with the experimental data.

However, using the more advanced approach of the next-neighbor model, which was used for the simulation of the coarsening of Ag islands by Morgenstern *et al.* in Ref. 31, was not successful in our case. The reason is that this approach requires the distances between the islands to be much larger than the island sizes. Since this is, contrary to the system simulated in Ref. 31, not the case for PTCDA/Ag(100), the approach failed.

For the best simulation of the experimental data we used a value for the prefactor  $D\rho_\infty/\ln \xi = 0.551 \pm 0.005$  s<sup>-1</sup> and a value for the island edge tension of  $\gamma = 44 \pm 5$  meV nm<sup>-1</sup>, which corresponds to an island edge tension per molecule  $\gamma^*$  of  $51 \pm 5$  meV, which we will discuss below.

From other independent measurements we determined a value for the surface diffusion constant at room temperatures  $D = 4.0 \times 10^3 \pm 1.1 \times 10^3$  nm<sup>2</sup> s<sup>-1</sup>.<sup>34</sup> Typical values for the screening length  $\ln \xi$  are about 2–3.<sup>7,32</sup> From these values we estimate a value for  $\rho_\infty \approx 3\text{--}4 \times 10^{-4}$  nm<sup>-2</sup>. Independently we measured the coverages of the molecules between the islands between  $\Theta = 0.0004$  and 0.02, depending on the exact location between the island.<sup>26</sup> These values correspond to a molecule densities of  $\rho = 3.1 \times 10^{-4}$  to  $1.5 \times 10^{-2}$  nm<sup>-2</sup>. The lower value corresponds well to the  $\rho_\infty$  value obtained from the above simulations. This is reasonable since  $\rho_\infty$  also refers to the thermodynamical lower limit of the molecular density which is present for an infinitely large island.

#### IV. FINAL DISCUSSION AND CONCLUSIONS

Coarsening on metal surfaces usually proceeds by two general mechanisms: Ostwald ripening (island decay) and Smoluchowski ripening (island or cluster coalescence).<sup>10,11,30</sup> Usually, for a given surface, one of these two scenarios is dominating. For example, for adatom islands on Ag(100) mostly coalescence can be observed, whereas the vacancy islands on the same surface undergo decay.<sup>1</sup> The coalescence proceeds only by the presence of cluster diffusion. For metal islands, cluster diffusion has been studied on various surfaces.<sup>10,12,13,17,28</sup> For PTCDA on Ag(100) we could not observe any island diffusion and subsequent coalescence. Island diffusion is mediated by *periphery diffusion* around the

island edge.<sup>1</sup> The absence of long-range island diffusion hence implies an existence of a large kink Ehrlich-Schwoebel barrier.<sup>1,30</sup>

The island decay of PTCDA on Ag(100) is clearly diffusion limited. This means that there exists no additional barrier larger than the diffusion barrier, when a PTCDA molecule moves from the position at an island edge to the next possible adsorption site on the terrace. This result is not trivial since it means that there is no additional activation barrier for molecules attaching at an island edge. The existence of such a barrier could have been anticipated, e.g., in form of a structural distortion which the molecules undergo upon adsorption into the ordered lattice of the island. In particular, it was observed for PTCDA on the Ag(111) surface that the molecules are slightly distorted from the planar geometry with the carboxylic O atoms lowered to the Ag surface due to the chemical bonding of the molecule to the surface.<sup>35</sup> The details of the distortion were in addition found to depend on the environment of the molecule, i.e., they differ for a molecule in an ordered and a disordered phase.<sup>25</sup> Such a distortion was recently also found for the ordered phase of PTCDA on Ag(100).<sup>36</sup> It is hence conceivable that a similar difference in the structural distortion exist here, too. Obviously, this difference is too small to yield a relevant interfacial barrier. Notably, an interfacial barrier was derived for rubrene island on sapphire from their decay kinetics.<sup>21</sup> The reason for this barrier might be structural distortion of the isolated rubrene molecule in contrast to that in the crystalline phase.<sup>37</sup>

The obtained value of the island edge line tension  $\gamma^*$  per molecule of  $51 \pm 6$  meV is of some basic interest. For a comparison, typical values for the comparable step line tension for metal atoms are 10–700 meV per atom obtained from various experimental measurements or theoretical calculations.<sup>2</sup> Although the value for  $\gamma^*$  refers to the average over all island edges, we may try a structural interpretation since the well-defined straight island edges are strongly prevailing here. As to be seen in the inset in Fig. 4(a), each molecule within an island is bonded to four neighbor mol-

ecules. At a step edge, one neighbor molecule is missing. Assuming only next-neighbor interactions, the line tension per molecule should hence amount to half of the attractive intermolecular next-neighbor interaction energy  $E_{NN}$ . Hence we estimate a value of  $E_{NN} = 2\gamma^* = 102 \pm 10$  meV. As described in the introduction, this interaction comprises electrostatic and substrate mediated components. Any quantitative comparison with intermolecular interactions within the PTCDA bulk crystal phase or on other surfaces, e.g., Ag(111) have to be considered with large care, since the bonding distances between the molecules on Ag(100) are determined by the commensurability of the substrate. To our knowledge, comparable values for other molecular adsorbates have not been reported so far. Nevertheless, the determined value constitutes an interesting test parameter for theoretical investigations on such systems, e.g., as recently performed by DFT calculations.<sup>38</sup>

Finally, we note that the possibility to obtain information about intermolecular interaction of large organic adsorbates on surfaces via the ripening kinetics is highly attractive. For atoms or small molecules, intermolecular interactions are traditionally determined from simulations of the respective phase diagrams of ordered structures.<sup>39</sup> In particular the transitions of the ordered phases to the disordered gas phases at high temperature contain information on the size of the adsorbate-adsorbate interactions. For organic adsorbates this access is often not possible, since the phase boundaries to the disordered phases cannot be reached, because the molecules desorb or dissociate at higher temperatures. This is also the case for PTCDA/Ag(100).<sup>23</sup> Hence the here described route constitutes a valuable alternative to obtain the interaction energies.

#### ACKNOWLEDGMENTS

We thank K. Morgenstern for valuable advice. This work was supported by the Deutsche Forschungsgemeinschaft (DFG) through the research center 624 “Chemical Templates.”

\*Corresponding author; ikonov@uni-bonn.de

<sup>1</sup>P. A. Thiel, M. Shen, D.-J. Liu, and J. W. Evans, *J. Phys. Chem. C* **113**, 5047 (2009).

<sup>2</sup>M. Giesen, *Prog. Surf. Sci.* **68**, 1 (2001).

<sup>3</sup>G. Witte and C. Wöll, *J. Mater. Res.* **19**, 1889 (2004).

<sup>4</sup>S. R. Forrest, *Chem. Rev.* **97**, 1793 (1997).

<sup>5</sup>*Organic Electronics*, edited by H. Klauk (Wiley-VCH, Weinheim, 2006).

<sup>6</sup>B. K. Chakraverty, *J. Phys. Chem. Solids* **28**, 2401 (1967).

<sup>7</sup>P. Wynblatt and N. A. Gjostein, in *Progress in Solid State Chemistry*, edited by J. O. McCardin and G. Somorjai (Pergamon, Oxford, 1975), Vol. 9, p. 21.

<sup>8</sup>N. C. Bartelt, W. Theis, and R. M. Tromp, *Phys. Rev. B* **54**, 11741 (1996).

<sup>9</sup>W. Theis, N. C. Bartelt, and R. M. Tromp, *Phys. Rev. Lett.* **75**, 3328 (1995).

<sup>10</sup>W. W. Pai, A. K. Swan, Z. Zhang, and J. F. Wendelken, *Phys. Rev. Lett.* **79**, 3210 (1997).

<sup>11</sup>C. R. Stoldt, C. J. Jenks, P. A. Thiel, A. M. Cadilhe, and J. W. Evans, *J. Chem. Phys.* **111**, 5157 (1999).

<sup>12</sup>J. M. Wen, S. L. Chang, J. W. Burnett, J. W. Evans, and P. A. Thiel, *Phys. Rev. Lett.* **73**, 2591 (1994).

<sup>13</sup>J. M. Wen, J. W. Evans, M. C. Bartelt, J. W. Burnett, and P. A. Thiel, *Phys. Rev. Lett.* **76**, 652 (1996).

<sup>14</sup>K. Morgenstern, G. Rosenfeld, and G. Comsa, *Phys. Rev. Lett.* **76**, 2113 (1996).

<sup>15</sup>K. Morgenstern, G. Rosenfeld, E. Lægsgaard, F. Besenbacher, and G. Comsa, *Phys. Rev. Lett.* **80**, 556 (1998).

<sup>16</sup>K. Morgenstern, G. Rosenfeld, G. Comsa, M. R. Sørensen, B. Hammer, E. Lægsgaard, and F. Besenbacher, *Phys. Rev. B* **63**, 045412 (2001).

<sup>17</sup>K. Morgenstern, G. Rosenfeld, B. Poelsema, and G. Comsa,

- Phys. Rev. Lett.* **74**, 2058 (1995).
- <sup>18</sup>H. Mehl, O. Biham, I. Furman, and M. Karimi, *Phys. Rev. B* **60**, 2106 (1999).
- <sup>19</sup>P. Stoltze, *J. Phys.: Condens. Matter* **6**, 9495 (1994).
- <sup>20</sup>Y.-R. Ma, P. Moriarty, and P. H. Beton, *Phys. Rev. Lett.* **78**, 2588 (1997).
- <sup>21</sup>P. Rebernik Ribič and G. Bratina, *J. Phys. Chem. C* **111**, 18558 (2007).
- <sup>22</sup>H. Marchetto, U. Groh, T. Schmidt, R. Fink, H. J. Freund, and E. Umbach, *Chem. Phys.* **325**, 178 (2006).
- <sup>23</sup>J. Ikononov, O. Bauer, and M. Sokolowski, *Surf. Sci.* **602**, 2061 (2008).
- <sup>24</sup>A. Kraft, R. Temirov, S. K. M. Henze, S. Soubatch, M. Rohlfiing, and F. S. Tautz, *Phys. Rev. B* **74**, 041402(R) (2006).
- <sup>25</sup>L. Kilian, A. Hauschild, R. Temirov, S. Soubatch, A. Schöll, A. Bendouan, F. Reinert, T.-L. Lee, F. S. Tautz, M. Sokolowski, and E. Umbach, *Phys. Rev. Lett.* **100**, 136103 (2008).
- <sup>26</sup>P. Bach, J. Ikononov, and M. Sokolowski (unpublished).
- <sup>27</sup>M. Wortis, *Chemistry and Physics of Solid Surfaces* (Springer, New York, 1988).
- <sup>28</sup>D. C. Schlößer, K. Morgenstern, L. K. Verheij, G. Rosenfeld, F. Besenbacher, and G. Comsa, *Surf. Sci.* **465**, 19 (2000).
- <sup>29</sup>G. Rosenfeld, K. Morgenstern, I. Beckmann, W. Wulfhekel, E. Lægsgaard, F. Besenbacher, and G. Comsa, *Surf. Sci.* **402-404**, 401 (1998).
- <sup>30</sup>J. Ikononov, K. Starbova, and M. Giesen, *Surf. Sci.* **601**, 1403 (2007).
- <sup>31</sup>K. Morgenstern, G. Rosenfeld, and G. Comsa, *Surf. Sci.* **441**, 289 (1999).
- <sup>32</sup>M. Zinke-Allmang, L. C. Feldman, and M. H. Grabow, *Surf. Sci. Rep.* **16**, 377 (1992).
- <sup>33</sup>G. Schulze Icking-Konert, M. Giesen, and H. Ibach, *Surf. Sci.* **398**, 37 (1998).
- <sup>34</sup>J. Ikononov, P. Bach, R. Merkel, and M. Sokolowski, *Phys. Rev. B* **81**, 161412(R) (2010).
- <sup>35</sup>A. Hauschild, K. Karki, B. C. C. Cowie, M. Rohlfiing, F. S. Tautz, and M. Sokolowski, *Phys. Rev. Lett.* **94**, 036106 (2005).
- <sup>36</sup>O. Bauer, Diploma thesis, University of Bonn, 2007).
- <sup>37</sup>D. Käfer, L. Ruppel, G. Witte, and Ch. Wöll, *Phys. Rev. Lett.* **95**, 166602 (2005).
- <sup>38</sup>M. Rohlfiing, R. Temirov, and F. S. Tautz, *Phys. Rev. B* **76**, 115421 (2007).
- <sup>39</sup>K. Binder and D. Landau, *Monte Carlo Calculations on Phase Transitions in Adsorbed Layers*, in *Advances in Chemical Physics*, edited by K. Lawley (Wiley, Chichester, 1989), Vol. 76, p. 91.